Rheol Acta (2004) 43: 657–669
DOI 10.1007/s00397-004-0405-4

ORIGINAL CONTRIBUTION

Martin L. Sentmanat

Miniature universal testing platform: from extensional melt rheology to solid-state deformation behavior

Received: 15 March 2004
Accepted: 15 June 2004
Published online: 12 August 2004

M. L. Sentmanat
Senkhar Technologies,
LLC, Akron, OH, USA
E-mail: mlsentmanat@aol.com

Abstract Described is a detachable fixture for a rotational rheometer, the Sentmanat Extensional Rheometer Universal Testing Platform, which incorporates dual wind-up drums to ensure a truly uniform extensional deformation during uniaxial extension experiments on polymers melts and elastomers. Although originally developed as an extensional rheometer, this highly versatile miniature test platform is capable of converting a conventional rotational rheometer host system into a single universal testing station able to characterize a host of physical properties on a variety of polymer melts and solid-state materials over a very wide range of temperatures and kinematic deformations and rates. Experimental results demonstrating these various testing capabilities are presented for a series of polymers of varying macrostructure and physical states.

Keywords Rotational rheometer · Uniform extensional deformation · Single universal testing station · Polymer melts · Solid-state materials · Extensional Rheometer

Introduction

Extensional flow, or deformation that involves the stretching of a viscous material, is the dominant type of deformation in converging and squeezing flows that occur in typical polymer processing operations. Although the extensional deformations experienced by polymers during processing are typically both large and rapid, characterizing the extensional flow behavior of polymers at these rates and deformations has historically been quite difficult. Nevertheless, despite the difficulty in conducting these experiments, extensional flow measurements are particularly useful in polymer characterization, because they are very sensitive to the molecular structure of the polymeric system being tested. When the true strain rate of extension, also referred to as the Hencky strain rate, is constant, simple extension is said to be a "strong flow" in the sense that it can generate a much higher degree of molecular orientation and stretching than flows in simple shear. As a consequence, elongational flows are very sensitive to crystallinity and macrostructural effects such as long-chain branching (LCB), and as such can be far more descriptive with regard to polymer characterization than other types of bulk rheological measurement.

Rheometers for characterizing the extensional flow behavior of polymer melts and elastomers have been described extensively in the literature [1, 2, 3, 4, 5, 6, 7, 8, 9, 10, 11]. The shortcomings of certain experimental methods with regard to extensional deformation control [12] and uniformity [13] have also been addressed in the literature. Due to limitations with the prior art, Sentmanat developed the dual wind-up extensional rheometer that takes advantage of the high strain and true applied strain rate capabilities of a fiber wind-up technique and addresses the issue of non-uniform deformations associated with fixed-ended fiber stretching. This patented technology [14, 15] employs a dual wind-up drum technique that allows the ends of a sample to be stretched by means of two counter-rotating

wind-up drums whose resistance to rotation is hindered by the material response of the stretching sample. Since dubbed the Sentmanat Extensional Rheometer, or SER for short, the commercial instrument exclusively manufactured by Xpansion Instruments has been designed for use as a detachable fixture on commercially available rotational rheometer host systems, and can be accommodated within the host's oven chamber to allow for the controlled temperature evaluation of materials [16, 17]. Although originally developed as a rheometer to be used for the extensional rheological characterization of uncured elastomers, this miniature unit requires only a few milligrams of material and has been designed in such a manner that it can be used for molten or solid materials characterization over a very wide range of temperatures and kinematic deformations and rates. As will subsequently be described, this fixture can convert a conventional rotational rheometer host system into a universal testing station capable of performing extensional melt rheology experiments, solids tensile testing, tear testing, t-peel/adhesion testing, high-speed cut growth testing, and dynamic friction testing, all within the controlled environment of the host system's environmental chamber.

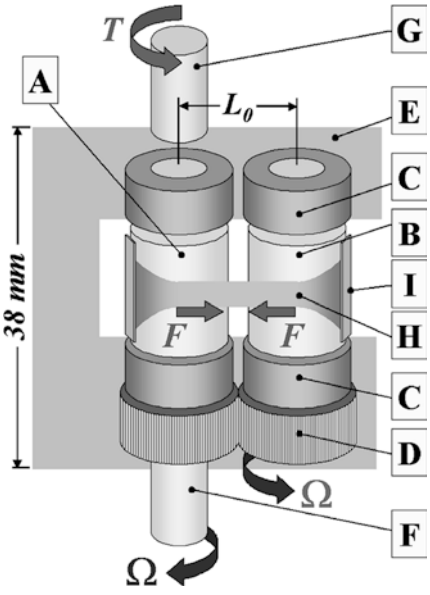

Fig. 1 Schematic view of the Sentmanat extensional rheometer (SER) during operation. Inside *squares: A* Master drum, *B* slave drum, *C* bearings, *D* intermeshing gears, *E* chassis, *F* drive shaft, *G* torque shaft, *H* sample, *I* securing clamps. Other symbols: L_0 unsupported length, Ω drive shaft rotation rate, *T* torque, *F* tangential force

Principle of operation

The rheometer consists of paired master, A, and slave, B, wind-up drums mounted on bearings, C, housed within a chassis, E, and mechanically coupled via intermeshing gears, D, as shown in Fig. 1. Rotation of the drive shaft, F, results in a rotation of the affixed master drum, A, and an equal but opposite rotation of the slave drum, B, which causes the ends of the sample, H, that are secured to the drums by means of securing clamps, I, to be wound up onto the drums resulting in the sample being stretched over an unsupported length, L_0. For a constant drive shaft rotation rate, Ω, the Hencky strain rate applied to the sample specimen can be expressed as:

$$\dot{\varepsilon}_{\mathrm{H}} = \frac{2\Omega R}{L_0} \tag{1}$$

where R is the radius of the equal dimension wind-up drums, and L_0 is the fixed, unsupported length of the specimen sample being stretched which is equal to the centerline distance between the master and slave drums.

The material's resistance to stretch is manifested as a tangential force, F, acting on both the master, A, and slave, B, drums. In the case of a rotational rheometer host system with a de-coupled drive motor (motor mount attached to drive shaft, F) and torque transducer (transducer mount attached to torque shaft, G), the stretching force acting on the master drum is borne by the drive shaft, F, and subsequently by the drive motor and contributes nothing to the resultant torque, T, borne by the chassis, E, and torque shaft, G. Ultimately the resultant torque, T, which is measured by the torque transducer, results only from the tangential stretching force acting on the slave drum, B. This is apparent from the following load analysis of the system.

Referring to Fig. 1 and Fig. 2, the tangential stretching force, F, on the slave drum is counteracted by the force, F', acting at the point of contact of the intermeshing gears. For a 1:1 gear ratio the intermeshing gear force F' can be resolved from a sum of moments about the slave drum's axis of rotatation, O' from Fig. 2, resulting in the following expression:

$$F' = \frac{(F + F_{\mathrm{F}})R}{L_0/2} \tag{2}$$

where F_{F} is any frictional force contribution that may exist from the gears and bearings. This force on the intermeshing gears, F', is then translated as a radial force on the bearings centered along the slave drum's axis of rotation, O' from Fig. 2. Since the torque shaft, G, is fixed to the chassis, E, along the master drum's axis of rotation, O from Fig. 2, a summation of moments about axis O yields the following expression:

$$T = F' L_0 \tag{3}$$

Substituting the expression from Eq. 2 into Eq. 3 yields the following:

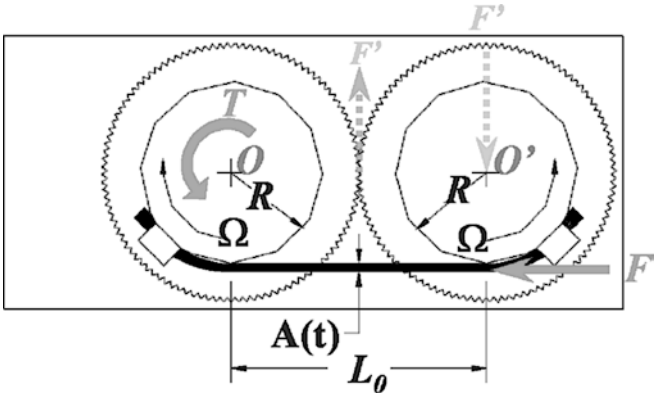

Fig. 2 Force diagram indicating the tangential stretching force, F, on the slave drum and the resultant torque, T, measured by the torque transducer of a de-coupled drive motor and torque transducer host system. Ω Drive shaft rotation rate, R radius, $A(t)$ instantaneous cross-sectional area, O sum of moments about the drum's axis of rotatation, F tangential force

$$T = 2(F + F_{\mathrm{F}})R \tag{4}$$

With the precision bearings and gears outfitted on the SER unit, the frictional term, F_{F}, is typically less than 2% of the stretch force, F, and can be neglected for torque values greater than 4.0e−5 Nm such that the expression for the measured torque can be simplified to

$$T = 2FR \tag{5}$$

Thus, in the case of a de-coupled drive motor and torque transducer host system, the SER chassis, E, serves merely as a pillow block for the drum bearings, C. By offsetting the slave drum's axis of rotation from the primary axis of rotation and utilizing a 1:1 gear ratio, a mechanical gain of two times the stretching force is elegantly achieved for any stretching/deformation operation.

If there is no deviation between the nominal and actual strain rates, the instantaneous cross-sectional area, $A(t)$, of the stretched specimen changes exponentially with time, t, for a constant Hencky strain rate experiment and can be expressed as:

$$A(t) = A_0 \exp\left[-\dot{\varepsilon}_{\mathrm{H}} t\right] \tag{6}$$

where A_0 is the initial cross-sectional area of the unstretched specimen. For a constant Hencky strain rate, the tensile stress growth function, $\eta_E{}^+(t)$, of the stretched sample can then be expressed as:

$$\eta_E^+(t) = \frac{F(t)}{\dot{\varepsilon}_{\mathrm{H}} A(t)} \tag{7}$$

where $F(t)$ is the instantaneous extensional force at time t exerted by the sample as it resists stretch as determined from the measured torque signal, T, and Eq. 5.

Materials and methods

Measurements were performed on a Xpansion Instruments SER Universal Testing Platform, model SER-HV-A01, specifically designed for use on a TA Instruments ARES or Rheometric Scientific ARES/RDA3/RDA2 rotational rheometer host system. The instrument's specifications are listed in Table 1. It should be noted that the maximum Hencky strain rate capability with the SER is limited only by the data acquisition and dynamic performance of the host rheometer system on which it is used. Although with proper care, Hencky strain rates of 30 s^{-1} and higher can be achieved with any of the aforementioned host systems, a maximum Hencky strain rate of 20 s^{-1} is recommended for applications in which the total test times are small (<0.1 s) and the stress evolution is critical, such as in tensile stress growth mode, due to inertial limitations associated with the transient torque response at very high rates of deformation.

Extensional rheology specimens were prepared by first compression-molding flat polymer samples to a nominal gage of less than 1 mm, and then cutting fixed width strips using a dual blade cutter. Thin-gage (0.1–0.15 mm) tensile specimens were also prepared by compression-molding. The ends of the specimen were loaded onto the securing clamps and sandwiched against the wind-up drums, thereby securing the ends of the sample for subsequent stretching. Because of the large stresses associated with solids tensile testing, a thin-gage (0.05–0.1 mm), double-sided adhesive tape was placed on the drum surfaces prior to specimen loading to prevent sample slippage during wind-up. Upon test completion, test specimens were immediately removed and the drums were carefully wiped clean with a soft

Table 1 Specifications for the SER-HV-A01 Universal Testing Platform

	Parameter	Specification
Instrument	Maximum operating torque	2,500 g-cm
	Minimum torque threshold	<0.2 g-cm
	Maximum recommended hencky strain rate	20 s^{-1}
	Maximum Hencky strain per drum revolution	4
	Operating temperature range	0–250 °C
	Windup drum diameter	1.031 cm (0.406 in)
	Stretch zone gage length	1.272 cm (0.501 in)
Sample	Min. recommended melt zero-shear viscosity (in extension mode)	~10,000 Pa s
	Sample mass range	5–200 mg
	Recommended sample width range	0.1–1.27 cm
	Recommended sample thickness range	0.005–0.1 cm

disposable laboratory wipe to remove any sample residue off the drum surfaces.

Results and discussion

Specimen dimensions and melt expansion

The width and thickness dimensions of the prepared polymer samples were measured at room temperature prior to loading on the SER. These dimensions were then used to establish the initial cross-sectional area, A_0, of the specimen prior to stretch. For melt rheology experiments however, polymer samples exhibit a decrease in density upon melting, manifested as a volumetric expansion of the specimen span while loaded on the SER. In order to account for this dimensional expansion the following expression was used to calculate the cross-sectional area of the molten polymer specimen:

$$A(t) = A_0\left(\frac{\rho_S}{\rho_M}\right)^{2/3}\exp\left[-\dot{\varepsilon}_H t\right] \tag{8}$$

where A_0 is the cross-sectional area of the specimen in the solid state, ρ_S is the solid-state density and ρ_M the melt density of the polymer. Note that the expansion in the unsupported span length of the polymer is observed as a slight lag in the torque response that can be accounted for with a slight time offset in the recorded time data. As demonstrated in the analysis contained in the Appendix, because of the SER's physical test geometry, specimen sag was found not to be an issue for polymer melts with a zero-shear viscosity of greater than 1.0e4 Pa s.

Strain validation

The validation of Hencky strain deformations during a steady uniaxial extension experiment with the SER-HV-A01 was achieved using digital videography to monitor the evolution of a specimen's width dimension at constant applied Hencky strain rates up to 20 s^{-1}. Assuming a no-slip condition on the surface of the wind-up drums, the theoretical width dimension of a rectangular cross-section specimen strip can be expressed by the following:

$$\frac{W(t)}{W_0} = \sqrt{\exp\left[-\varepsilon_H\right]} \tag{9}$$

where $W(t)$ is the instantaneous width dimension at time t, W_0 is the initial width dimension of the specimen prior to stretch, and ε_H is the total applied Hencky strain on the specimen. For a constant Hencky strain rate experiment, Eq. 9 can be rewritten as follows:

$$\frac{W(t)}{W_0} = \sqrt{\exp\left[-\dot{\varepsilon}_H t\right]} \tag{10}$$

Hence, recalling Eq. 1 for a uniaxial extension experiment the theoretical specimen width dimension is only a function of the applied drum rotation.

Figure 3 is a representative depiction of specimen width evolution for an uncured SBR elastomer at room temperature for an applied Hencky strain rate of 1.0 s^{-1} with the SER. Superposed over the actual image of the specimen undergoing stretch is the theoretical specimen width dimension according to Eq. 10 depicted as a box outline across the span of the stretch zone defined by the tangent line of the wind-up drums. Note the excellent agreement between the actual and theoretical specimen width evolution, even up to the point of specimen rupture. It should also be noted that uncured elastomers such as the one depicted in Fig. 3 readily exhibit slip in simple shear, even at very small deformations, often rendering conventional shear rheology methods ineffective as a means of material characterization. Nevertheless, despite this propensity for slip in simple shear, polymers such as the one depicted in Fig. 3 exhibit no adverse effects to the extensional deformation applied by the SER.

Figure 4 displays the excellent superposition of actual and theoretical width evolution values obtained for a multitude of uncured elastomers and polymer melts at Hencky strain rates up to 20 s^{-1}, thereby illustrating the agreement between actual and applied strain with the SER over a broad range of extensional rates. As discussed previously, for cured elastomers and solid-state materials, the use of a thin-gage double-sided adhesive tape on the wind-up drum surfaces is recommended in order to prevent slippage and ensure the equality between actual and applied strain with the SER.

Validation with extensional rheology results from the literature

Uniaxial extension experiments were performed at ambient temperature (23 °C) on a commercial polyisobutylene(PIB) (BASF Oppanol B15) with a M_n of 44,000 and a M_w of 88,000. This same material was characterized in uniaxial extension experiments by other independent laboratories using different types of extensional rheometer as published in the literature [18, 19]. Figure 5a, b, c contains the tensile stress growth curves obtained with the SER superposed over the stress growth data reported in the other studies at Hencky strain rates of 0.05, 0.08, and 0.12 s^{-1}, respectively. Note the agreement between the SER data and the data obtained from the other laboratories utilizing a variety of extensional rheometer technologies.

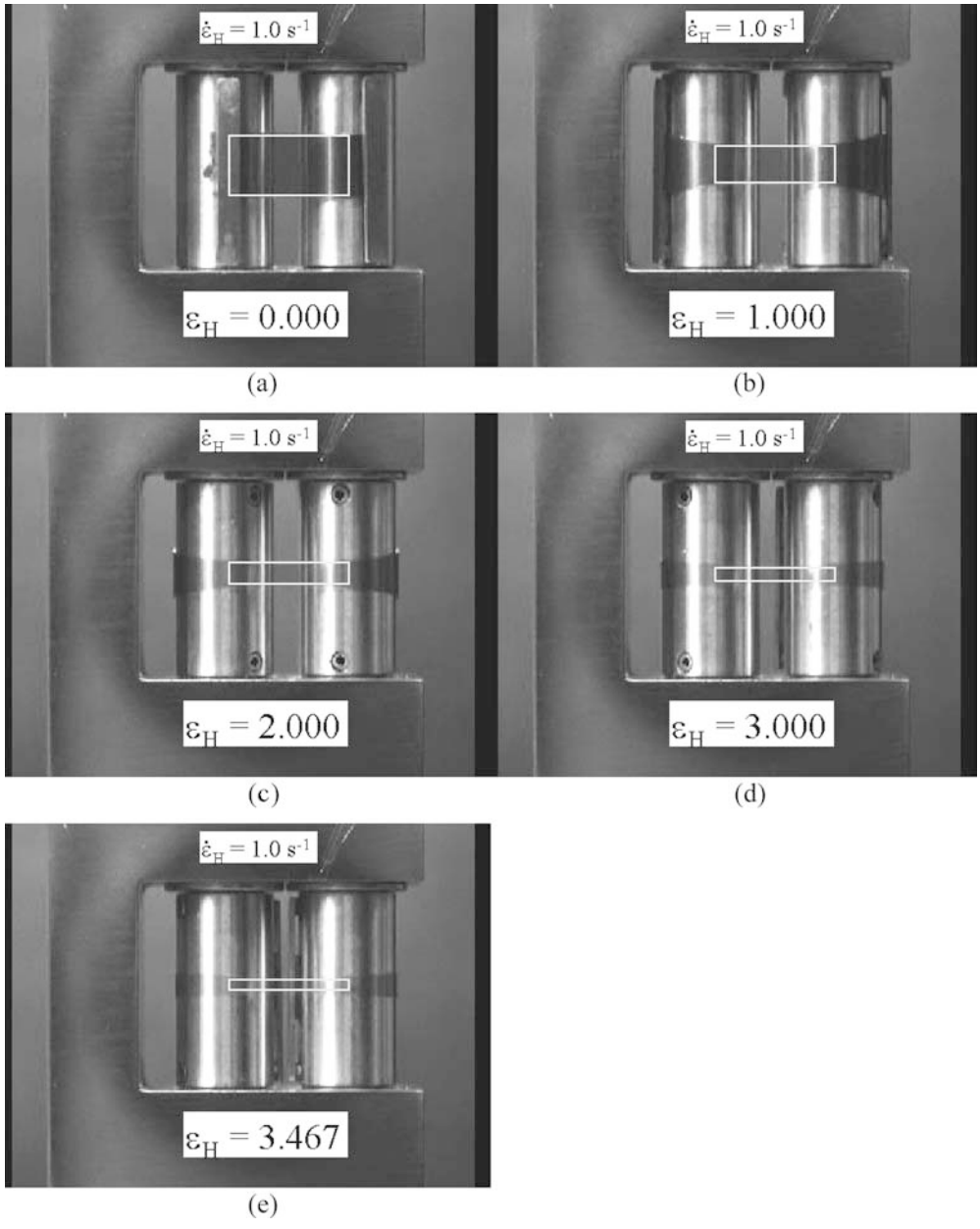

Fig. 3a–e Stop-frame videographic sequence depicting the evolution of an extensional rheology specimen's width dimension at an applied Hencky strain rate of 1.0 s^{-1} with the SER-HV-A01 superposed with the theoretical width dimension (depicted as a box outline) based solely on drum rotation from **a** test initiation to **e** the moment immediately prior to sample rupture. ε_H Hencky strain

Transient extensional experiments were also performed on a low-density polyethylene (LDPE) melt (BASF Lupolen 1840H, courtesy of Prof. Gareth McKinley of MIT) with a M_n of 17,000, a M_w of 240,000, and a CH_3/1,000C of 23 at a melt temperature of 150 °C. This same material was also characterized in uniaxial extension at the same temperature with an extensional rheometer developed by Münstedt [20]. Figure 6 contains a plot of the tensile stress growth function versus applied Hencky strain obtained with the SER superposed with Münstedt's data at Hencky strain rates of 0.1, 0.5, and 1 s^{-1}. Note the excellent agreement in the two independent sets of uniaxial extension melt data, which further demonstrates the veracity and control of the extensional deformation achieved with the SER. Further extensional melt rheology results with the SER and this LDPE material are the focus of a concurrent study [17].

Extensional rheology experiments with natural rubber

Uncured natural rubber is an extremely resilient, strain-crystallizing polymer that can be very difficult to characterize rheologically, particularly at room temperature. As a consequence, the linear viscoelastic

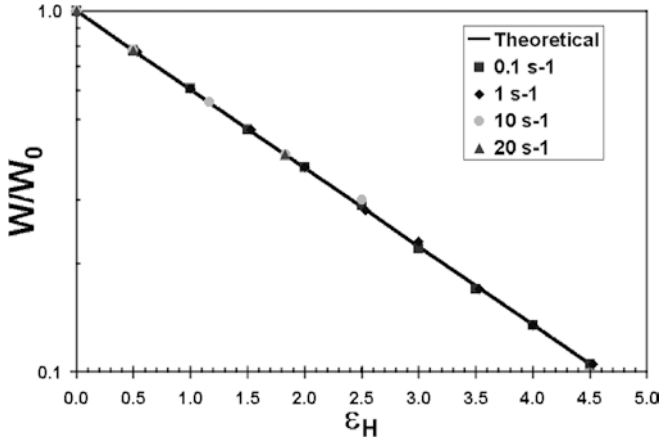

Fig. 4 Strain validation plot for the SER-HV-A01 Universal Testing Platform measured with a multitiude of materials at Hencky strain rates up to 20 s^{-1}

Fig. 5a–c Comparison of tensile stress growth curves obtained with the SER and data from the literature [18, 19] for the same commercial polyisobutylene (PIB) at room temperature for Hencky strain rates of **a** 0.05 s^{-1}, **b** 0.08 s^{-1}, and **c** 0.12 s^{-1}

(LVE) properties of natural rubber that are typically characterized in simple shear, can be very difficult to obtain due to the ever present effects of slip associated with simple shear experiments. Although the LVE shear stress relaxation modulus, $G(t)$, of natural rubber at room temperature may be difficult to directly determine without the use of sample/rheometer fixture bonding, the LVE extensional stress relaxation modulus, $E(t)$ [$=3G(t)$], can be easily characterized from step extension experiments with the SER. Figure 7 is a plot of the LVE extensional stress relaxation modulus for a rib smoked sheet grade natural rubber (NR–RSS2) obtained at room temperature for a step Hencky strain of 0.2 with the SER.

Figure 8 contains a plot of the tensile stress growth curves for uncured NR-RSS2 at room temperature performed at constant Hencky strain rates ranging from 0.001 to 10 s^{-1}. Also included on the graph is a plot of the LVE stress relaxation modulus data from Fig. 7 integrated with respect to time, which from theory defines the LVE envelope of tensile stress growth behavior. Note the excellent agreement between the low-strain portions of the five tensile stress growth curves from steady extension experiments and the LVE envelope

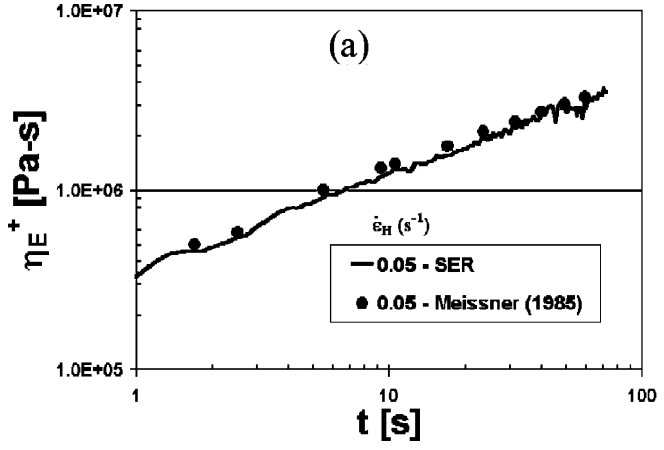

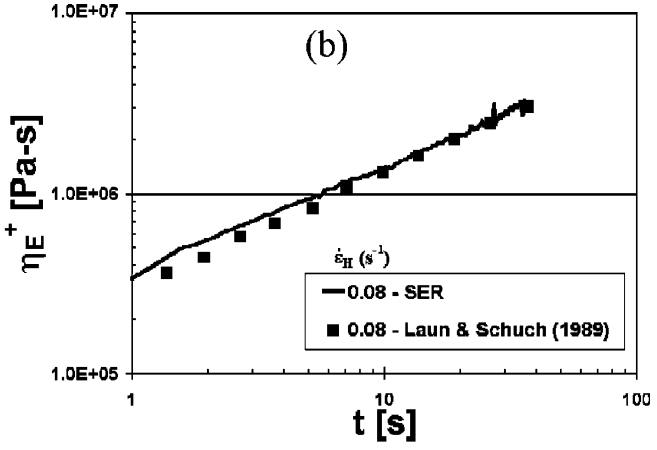

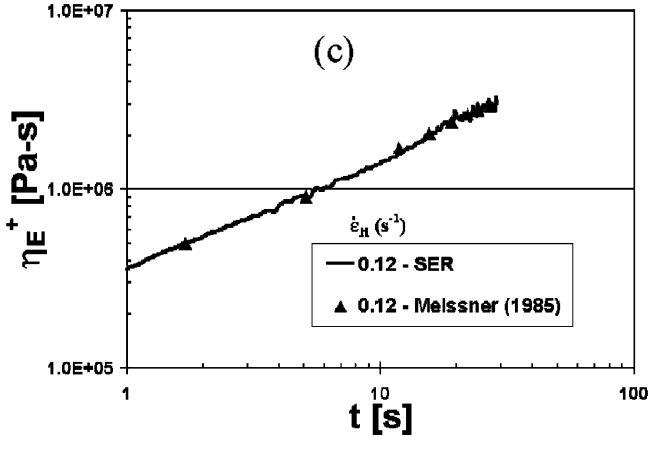

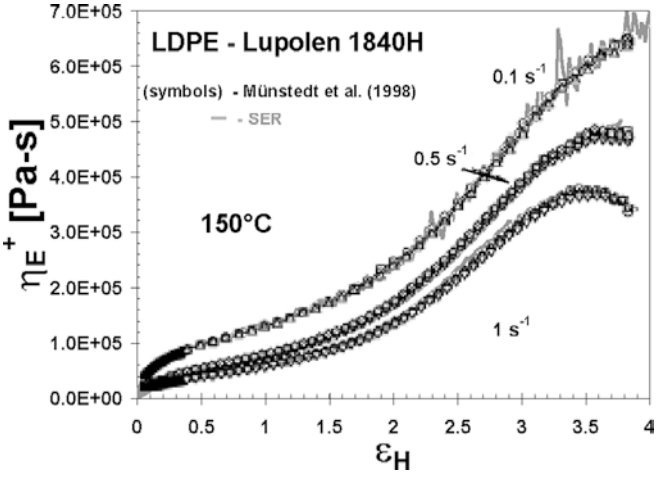

Fig. 6 Comparison of the tensile stress growth function versus Hencky strain curves obtained with the SER (*solid gray lines*) and data from the literature (*black symbols* from Münstedt et al. [20]) for the same low-density polyethylene (*LDPE*) (BASF Lupolen 1840H) at a melt temperature of 150 °C and for Hencky strain rates of 0.1 s^{-1}, 0.5 s^{-1}, and 1 s^{-1}

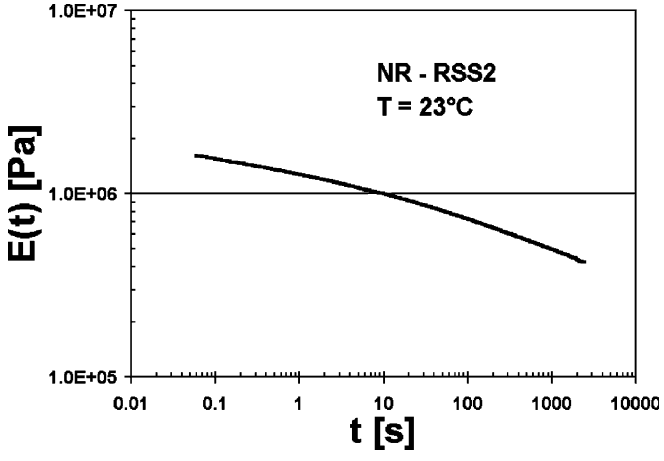

Fig. 7 Extensional stress relaxation modulus for NR-RSS2 for a step Hencky strain of 0.2 at 23 °C

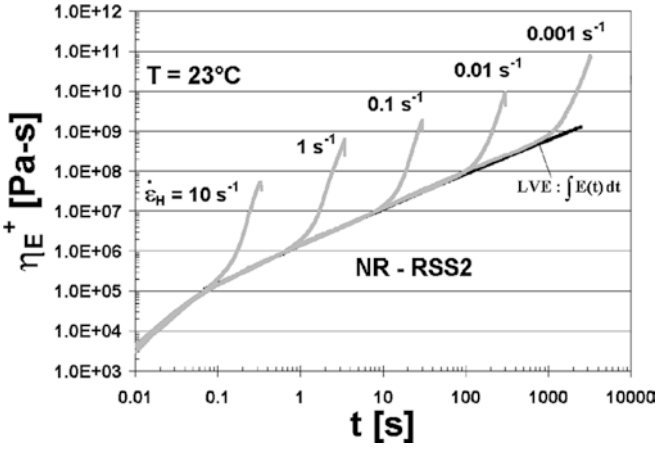

Fig. 8 Tensile stress growth curves for NR-RSS2 for constant Hencky strain rates ranging from 0.001 to 10 s^{-1}

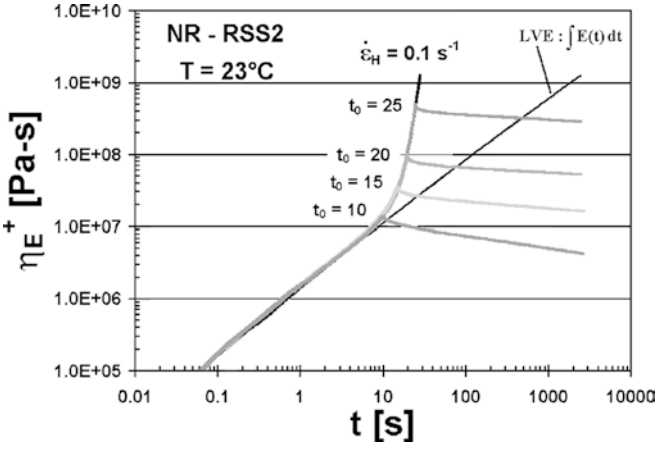

Fig. 9 Cessation of steady extension curves for NR-RSS2 at 23 °C for a steady Hencky strain rate of 0.1 s^{-1} stopped at a test time, t_0, of 10, 15, 20, and 25 s. Note the excellent reproducibility of the growth curves. *LVE* Linear viscoelastic

data taken from the step extension experiment. The significant deviation from LVE behavior with increasing deformation is due to strain-induced crystallization behavior inherent to natural rubber at ambient temperature.

The effects of strain-induced crystallization on the stress relaxation behavior of NR-RSS2 can be characterized from cessation of steady extension experiments. Constant Hencky strain rate measurements at 0.1 s^{-1} were performed on four NR-RSS2 samples in which the extensional deformation was stopped after test times of 10, 15, 20, and 25 s, the results of which are shown in Fig. 9 superposed with the tensile growth curve data for an uninterrupted steady Hencky strain rate of 0.1 s^{-1}. Also depicted in Fig. 9 is a plot of the time integral of the extensional stress relaxation modulus defining the LVE envelope of tensile stress growth behavior. Note the excellent reproducibility in the stress growth data generated with the SER as reflected by the superposition of all five tensile stress growth curves prior to the cessation of extension. As indicated by the relative stress relaxation curves of Fig. 10, the extent of strain-induced crystallization acts to significantly retard the relaxation behavior of natural rubber, an experimental observation that is extremely difficult to determine in simple shear.

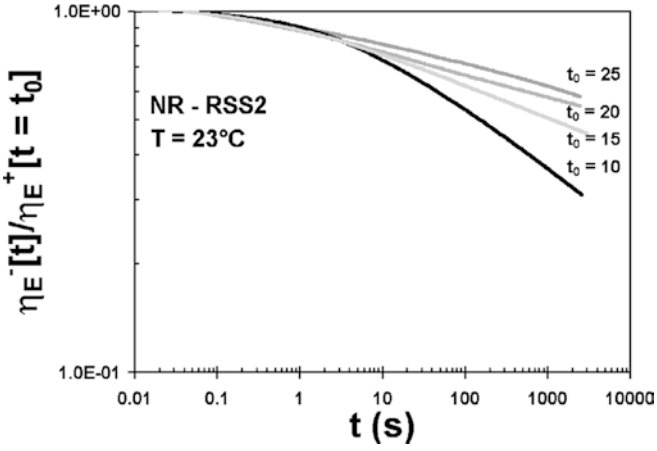

Fig. 10 Relative stress relaxation curves for NR-RSS2 at 23 °C from cessation of steady extension experiments demonstrating the effect of strain-induced crystallization behavior on stress relaxation

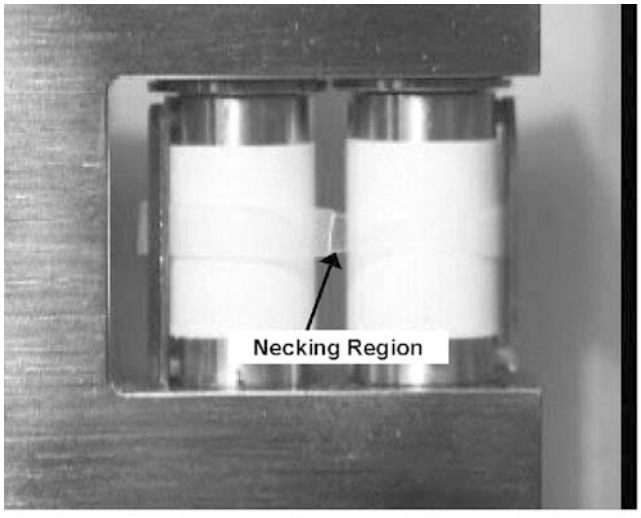

(a)

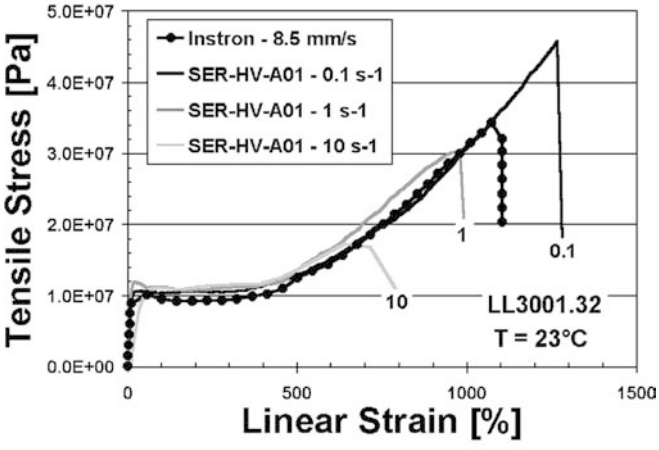

(b)

Fig. 11 **a** Photographic image of a solid LL3001.32 specimen undergoing tensile deformation and necking behavior on the SER. **b** Tensile curves for LL3001.32 at 23 °C generated with the SER at Hencky strain rates from 0.1 to 10 s^{-1} superposed with Instron tensile data for a rate of 8.5 mm s^{-1}

Detecting differences between linear and branched polymers

As an exercise to evaluate the SER's ability to distinguish macrostructural differences between polymers of similar microstructure, linear and branched commercial polymers were acquired for the purposes of study. The linear polymer was a film grade linear LDPE (LLDPE) (LL3001.32 from ExxonMobil Chemicals) with a melt flow index (MFI) = 1.0, while the branched polymer was a coating grade LDPE (LD200 from ExxonMobil) with a MFI = 7.5. With the exception of general information from the commercial product datasheets, nothing else was known about these polymers with regard to molecular weight, distribution, degree of branching or branching type prior to testing. Hence, this exercise was similar to the types of ''blind'' polymer characterization studies commonly encountered and requested of industrial research scientists.

Although originally developed as an extensional rheometer for uncured polymers and melts, the SER is capable of adeptly performing tensile testing on thin-gage solid materials, as shown in Fig. 11a. In Fig. 11b and Fig. 12 are shown engineering tensile stress versus engineering strain plots for solid polyethylene specimens of LL3001.32 and LD200, respectively, for a range of Hencky strain rates from 0.1 to 10 s^{-1}. Included in Fig. 11b and Fig. 12 are Instron tensile data obtained at a standard crosshead speed of 8.5 mm/s (20 in/min). The superposition of the SER and Instron tensile data curves is an indication of the agreement between the applied and actual strains of deformation with the SER for these high-modulus materials. Additionally, the SER data are able to capture the same yield, necking, and strain crystallization behavior observed with the data from conventional tensile testing methods. The SER results also reveal the influence of deformation rate on material strength particularly for the LL3001.32 polymer, in which it appears that crystallization kinetics are the limiting factor with regard to tensile strength behavior prior to material rupture. It is also worth noting that the SER's results for a 0.1 s^{-1} Hencky strain rate, which approximately corresponds to the initial diminishing Hencky strain rate witnessed by a standard tensile specimen at this constant crosshead speed, appear to suggest a premature rupture condition with the Instron samples. This observation is attributed to the large stress concentration associated with the sample grips of conventional tensile testing apparatus. As a result of this stress concentration, tensile specimens often rupture at a

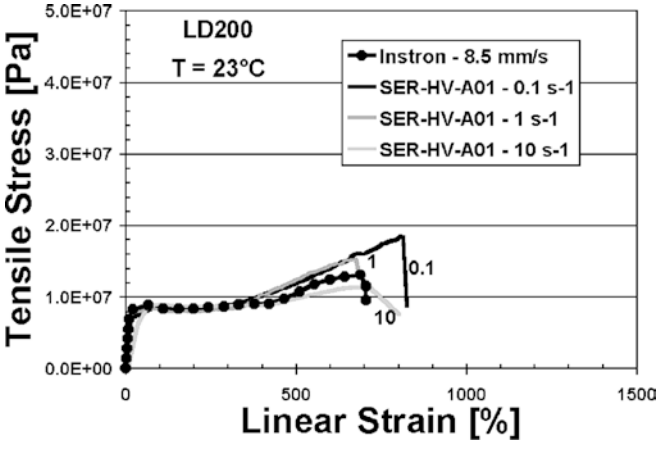

Fig. 12 Tensile curves for LD200 at 23 °C generated with the SER at Hencky strain rates from 0.1 to 10 s^{-1} superposed with Instron tensile data for a rate of 8.5 mm s^{-1}

location very near the grip region of the conventional tensile test specimen. It is believed that the SER tensile data reflect a truer characterization of a material's physical properties due to the lack of such stress singularities associated with sample gripping. Nevertheless, despite the notable difference in tensile behavior between the LL3001.32 and LD200 polymers, very few conclusions can be definitively drawn from the tensile data with regard to LCB and molecular weight characteristics.

LVE small amplitude oscillatory shear (SAOS) frequency sweep experiments were performed on the two polymers at a temperature of 150 °C, the results of which are included in Fig. 13a. Without having prior knowledge of the polymers' general macrostructural architectures, it is very difficult to distinguish LCB effects from molecular weight distribution effects based solely on the SAOS results. Likewise, LVE shear stress relaxation results don't provide definitive evidence with regard to the polymer LCB effects, as witnessed by the relaxation curves shown in Fig. 13b. As demonstrated by this data in simple shear, a LVE rheological characterization alone is often insufficient to distinguish between macrostructural features such as LCB and molecular weight distribution without having knowledge of these a priori.

In order to evaluate its capabilities in the LVE regime, extensional stress relaxation experiments with the SER, historically difficult measurements to execute, were performed on the polymer melts at a temperature of 150 °C and a step Hencky strain of 0.2. As shown in Fig. 14, a plot of the extensional stress relaxation modulus, $E(t)$, for each polymer is nearly identical to a plot of $3G(t)$ taken from the simple shear data of Fig. 13b, an experimental validation of Trouton's rule in stress relaxation mode. Although this LVE rheological characterization again fails to provide conclusive evidence with regard to LCB, the excellent agreement between the LVE simple shear data and the LVE extensional melt data taken with the SER is noteworthy.

Unlike the LVE experimental results, the tensile stress growth curves shown in Fig. 15 are far more descriptive as they depict the linear and non-linear viscoelastic behaviors as well as the rupture characteristics of the polymer melts. The agreement between the low-strain portions of the tensile stress growth curves and the LVE $3\eta^{+}(t)$ shear stress growth data taken from cone and plate measurements in start-up of steady shear is noteworthy. This is a valuable observation in that the same LVE information typically reserved for simple shear characterization techniques can be extracted from the LVE envelope from the low-strain tensile stress growth data. At long times, the LVE data indicate that the LL3001.32 polymer has a zero-shear viscosity almost 2.5 times that of the LD200 polymer, an observation that is consistent with the LVE results in simple shear.

Fig. 13 Melt data in simple shear for LD200 and LL3001.32 at 150 °C. **a** Dynamic shear modulus data from small amplitude oscillatory shear experiments. **b** Shear stress relaxation modulus from step shear experiments

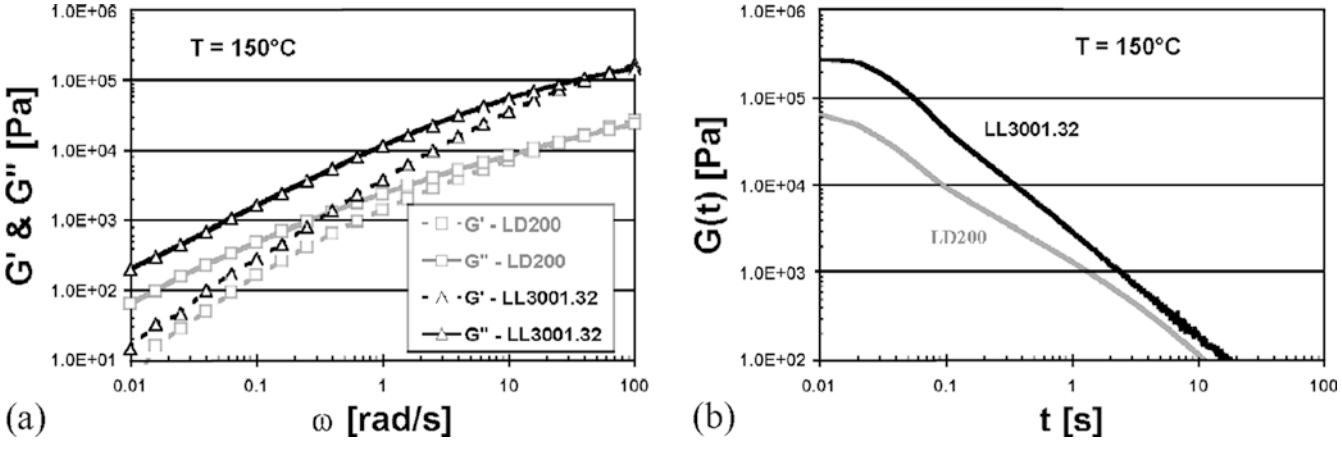

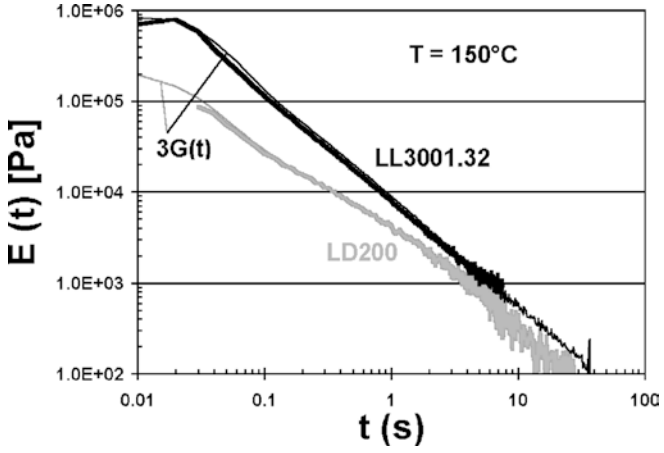

Fig. 14 LVE extensional stress relaxation modulus curves for LD200 and LL3001.32 at 150 °C superposed with the curves of $3G(t)$ for each polymer taken from the shear data in Fig. 17b

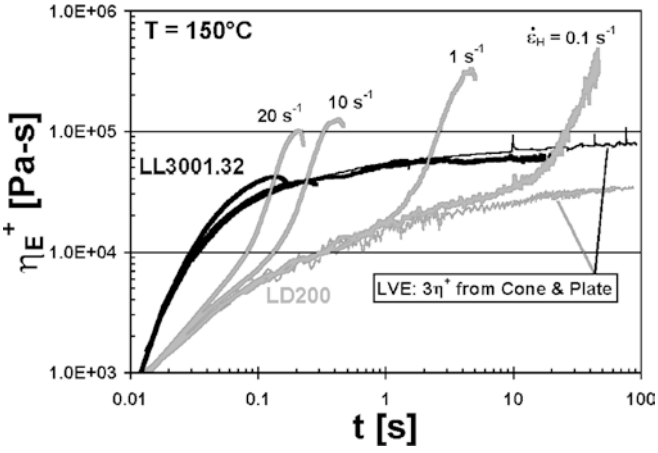

Fig. 15 Tensile stress growth curves for LD200 and LL3001.32 at 150 °C superposed with the LVE $3\eta^+(t)$ shear stress growth curves for each polymer taken from cone and plate measurements in start-up of steady shear at 150 °C

At high strains beyond the LVE envelope, the data is far more discriminating. Despite exhibiting a much lower LVE and melt flow viscosity, the LD200 exhibits peak stresses about three to five times higher than the LL3001.32 melt. With the exception of the highest Hencky strain rate data the LL3001.32 melt exhibits no significant deviation from LVE behavior whereas the LD200 melt exhibits significant strain-hardening attributed to polymer backbone stretch [21], an observation that is consistent with the extensional behavior of similar LCB polyethylenes [20]. The fact that for both materials combined, all of the tensile stress growth data in Fig. 15 required little more than 1 g of sample and took less than an hour to characterize is an indication that the SER offers an efficiently rapid yet accurate means of extensional melt flow characterization that is useful in distinguishing polymer LCB.

Additional testing capabilities

Although the preceding results demonstrate the versatility of an instrument capable of characterizing the large-scale uniaxial extension behavior of a material from its solid state to its melt state, as a testing platform the SER is not just limited to uniaxial deformation applications. The SER is also capable of performing peel/adhesion measurements as shown in Fig. 16a for characterizing the peel strength of adhesives, gels, pastes, and melts against a variety of thin-film substrates and over a broad range of rates and temperatures. Figure 16b contains peel strength curves for a general-purpose transparent adhesive tape versus plain white copier paper over a range of peel rates from 0.001 cm/s to 100 cm/s and at test temperatures of 23 °C and 50 °C. The peel data reveal that over a certain temperature-dependent range of peel rates, the peel strength of the tape is almost constant as one might expect of a general-purpose adhesive tape. Note as well that at very large peel rates, the adhesive strength of the tape increases to the point of cohesive paper failure as exhibited by the room temperature peel data at 100 cm/s. The SER offers significant advantages over conventional peel-testing methods in that the peel specimen sizes are small (< 10 mg), adhesion strength can be characterized as a function of environment over a very broad range of rates, the interfacial peel plane remains fixed for visualization accessibility (as depicted in Fig. 16a), and the legs of the t-peel specimen are supported during the measurement, thereby minimizing the leg stretch deformation contributing to the peel force response. Peel results with the SER that provide fundamental insight into polymer processing behavior for a series of polyethylene melts are the subject of a concurrent study [22].

With deadweight and a special free-pivoting friction armature that attaches to the side of the SER chassis as shown in Fig. 17a, a specimen can be pressed in a controlled manner against the bare surface of the slave drum or against a thin film/substrate wrapped around the slave drum. By controlling the rotational rate of the slave drum and monitoring the resultant torque on the slave drum, the dynamic slip/friction properties of solid polymers and elastomers can be easily evaluated as functions of contact media, rate, normal force, and temperature. Figure 17b provides an illustration of the reproducibility of room temperature dynamic friction coefficient traces for a TPE polymer sample against a dry, smooth polyester film substrate at a sliding speed of 2.5 mm/s (0.1 in/s) and a normal force of 1.33 N. The SER offers significant advantages over conventional friction testing methods in that the friction specimen

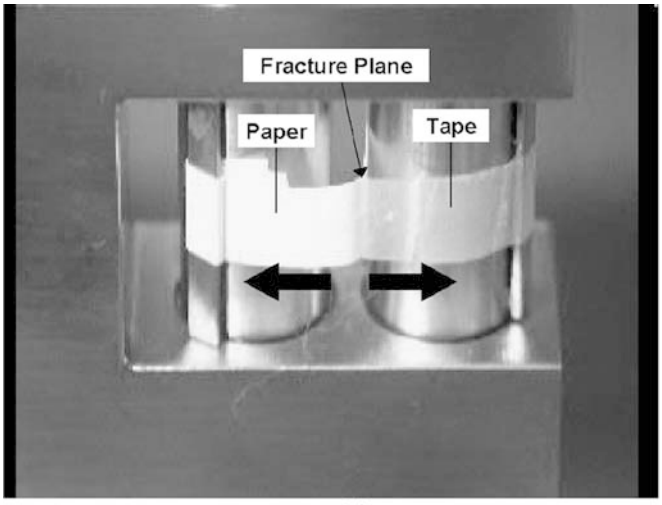

(a)

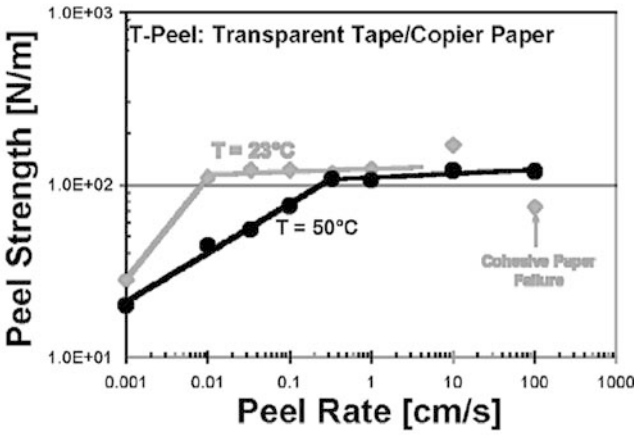

(b)

Fig. 16a, b T-peel experiments with the SER. **a** Photo image of a t-peel tear test with a general purpose transparent adhesive tape versus white stock copier paper. **b** Peel strength curves for transparent tape versus paper t-peel specimens over a range of peel rates from 0.001 to 100 cm s^{-1} and at temperatures of 23 °C and 50 °C

sizes are small (< 100 mg), that friction can be characterized as a function of environment over a broad range of rates, and that the interfacial friction plane remains fixed for visualization accessibility (as depicted in Fig. 17a).

Fig. 17a, b Dynamic friction experiments with the SER. **a** Photo image of the SER with the friction armature attachment and a loaded sample for dynamic friction testing. **b** Reproducibility of several friction coefficient traces for TPE versus a dry, smooth polyester film at a surface speed of 2.5 mm s^{-1} and at a temperature of 25 °C

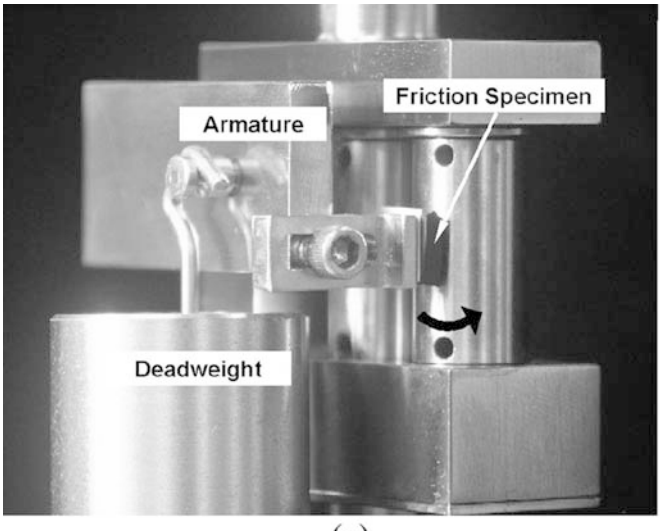

(a)

As described elsewhere [23], the SER is also capable of characterizing the tear strength and high-speed cut growth/fracture behavior of solid materials under controlled temperature and at very high applied rates in excess of 100 cm/s.

Conclusions

Features of a novel instrument for characterizing the extensional rheological behavior of polymeric materials as well as a host of other physical material properties were described. Designed as a detachable fixture for a rotational rheometer host system, the SER Universal Testing Platform incorporates dual wind-up drums that ensure a truly uniform extensional deformation during uniaxial extension experiments. Videographic analyses of polymer specimen width evolution demonstrated the

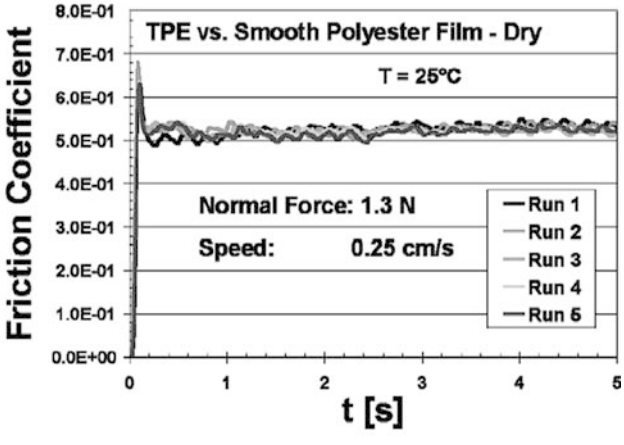

(b)

SER's ability to apply a uniform and controlled deformation during steady uniaxial extensional deformations for Hencky strain rates up to 20 s^{-1}. Extensional rheology results with the SER for a commercial PIB and a LDPE melt exhibited excellent agreement with similar results taken from the literature. LVE stress relaxation, steady uniaxial extension, and cessation of steady extension results were presented for a natural rubber revealing the effects of strain-induced crystallization on tensile stress growth and relaxation behavior. LVE extensional stress relaxation results for two polyethylene melts at 150 °C exhibited excellent agreement with stress relaxation data taken in simple shear. Tensile stress growth curves for LLDPE and LDPE melts at 150 °C demonstrated the utility of extensional rheology with the SER in distinguishing macrostructural features such as polymer LCB. Although originally developed as an extensional rheometer to be used for the rheological characterization of uncured polymers and melts, additional modes of operation were also described for this robust instrument demonstrating the SER's ability to perform tensile, peel, and friction testing on polymeric materials under a controlled temperature environment.

Acknowledgements The author would like to gratefully acknowledge Xpansion Instruments, LLC for granting access to the use of their equipment and Prof. Gareth McKinley of MIT for providing the BASF Lupolen 1840H material for extensional flow characterization. Extreme gratitude is also expressed to Prof. Savvas Hatzikiriakos of the University of British Columbia and Prof. John M. Dealy and post-doctoral fellow Dr. Chunxia He of McGill University for their helpful discussions during the preparation of this manuscript.

Appendix

Extensional melt rheology and specimen sag

As is the case with any melt rheometer device, unsupported molten polymer may have a tendency to sag owing to the effects of gravity acting on the mass of the sample. These sag effects may be particularly acute for extensional melt rheometers where spans of molten polymer sample are inherently unsupported. Prior extensional rheometer technologies in the literature have attempted to counteract the effects of sag by the use of either an oil bath environment or a pressurized gas cushion to buoy the sample during stretching. However, with proper design of the sample and testing geometry, these buoying techniques may be obviated for polymer melts with relatively low zero-shear viscosity.

To illustrate, consider the case of a uniaxial extension specimen geometry in which the primary axis of extensional deformation lies in the horizontal plane. The specimen geometry can be modeled as a uniform cross-section, simply supported beam span such as the one depicted in Fig. 18a. As a first approximation, specimen sag may be modeled as a classic beam flexure analysis for a concentrated load (the beam's weight) at the beam's mid-span. Hence, the beam deflection or amount of specimen sag, y, can be expressed as:

$$y = -\frac{mgL_0^3}{48EI} \tag{11}$$

where m is the specimen's free span mass, g is the gravitational constant, L_0 is the specimen span length, E is the characteristic elastic modulus of the specimen at a given melt temperature, and I is the beam's moment of inertia, a function of the specimen's cross-sectional geometry. The specimen's free-span mass is simply equal to the melt density, ρ_M, multiplied by the free-span volume ($m = \rho_M L_0 A$ where A is the cross-sectional area of specimen). At very low rates of beam deflection typical with polymer sag dynamics, the characteristic elastic modulus E is expected to be a function of the polymer's zero-shear viscosity η_0. Making use of the generalized expressions for solid and fluid tensile stress, σ_E, the following expression can be written:

$$\sigma_E = E\varepsilon = 3\eta_0\dot{\varepsilon} \tag{12}$$

In the limits of small deformations and rates, the following assumption can be made with regard to the rate of deformation:

$$\dot{\varepsilon} \approx \frac{\varepsilon}{t} \tag{13}$$

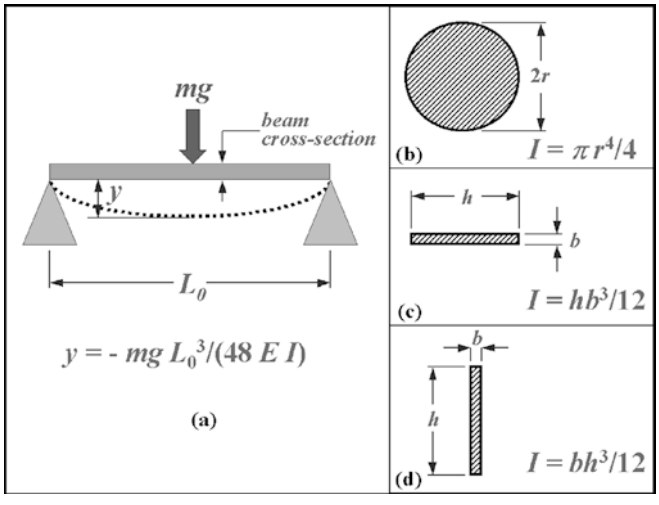

Fig. 18a–d Simply supported beam deflection diagram for a mid-span beam weight concentration (**a**) and the corresponding flexural moment of inertia, I, depicted for three types of beam cross section: **b** circular beam section, **c** flat rectangular beam section, and **d** upright rectangular beam section

such that the expression in Eq. 13 can be substituted into Eq. 12 and rearranged to arrive at an expression for the characteristic elastic modulus, E:

$$E = \frac{3\eta_0}{t} \tag{14}$$

where t is equal to the elapsed time of the beam deflection.

As depicted by the beam section geometries in Fig. 18b, c, d, the expression for the moment of inertia, I, is dependent on the cross-sectional beam dimensions with respect to the plane of specimen flexure. Substituting Eq. 14 and the corresponding expressions for m and I, Eq. 11 can be rearranged to obtain an expression for the rate of specimen sag, y/t, such that the following geometry-specific expressions may be written:

Figure 3b case (circular section): $$\frac{y}{t} = \frac{\rho_M g L_0^4}{36\eta_0 r^2} \tag{15}$$

Figure 3c case (flat rectangular): $$\frac{y}{t} = \frac{\rho_M g L_0^4}{12\eta_0 b^2} \tag{16}$$

Figure 3d case (upright rectangular): $$\frac{y}{t} = \frac{\rho_M g L_0^4}{12\eta_0 h^2} \tag{17}$$

Note that the rate of specimen sag scales with the span length raised to the fourth power and is inversely proportional to the square of the beam dimension height. Hence, for an illustrative scenario in which $h = 10$, $b = 20r$ and L_0 is fixed, a circular cross-section specimen will sag at a rate 133 times faster, and a flat rectangular cross-section specimen at a rate 100 times faster than an upright rectangular specimen, as in the case of an SER sample specimen. An analogous illustration of this result can be made by comparing the deflection of a single sheet of paper suspended flat at one end with the deflection of the same sheet of paper suspended upright on one edge. Thus, by placing a thin, wide specimen on its edge in an upright position as with the SER configuration (as in Fig. 18d), the effects of sag may be greatly reduced by making use of simple beam flexure mechanics.

References

1. Meissner J (1972) Trans Soc Rheol 16:405–420
2. Meissner J (1987) Recent Dev Polym Eng Sci 27:537–546
3. Cogswell FN (1968) Plastics Polym 36:109–111
4. Vinogradov GV, Leonov AI, Prokunin AN (1969) Rheol Acta 8:482–490
5. Macosko C, Lornston J (1972) SPE Tech Papers 19:461–467
6. Everage AE, Ballman RL (1976) J Appl Polym Sci 20:1137–1141
7. Connelly RW, Garfield LJ, Pearson GH (1979) J Rheol 23:651–662
8. Münstedt H (1979) J Rheol 23:421–436
9. Meissner J, Hostettler J (1994) Rheol Acta 33:1–21
10. Padmanabhan M, Kasehagen L J, Macosko C (1996) J Rheol 40:473–481
11. Carter R *et al* (2001) Polym Rheol Conf 2001 Tech Proc Paper 4:1–4
12. Wassner E (1999) Determination of true extensional viscosities with a Meissner-type rheometer (RME). In: Proceedings of the Polymer Processing Society 15th Annual Meeting, 's-Hertogenbosch, The Netherlands, p 66
13. Sentmanat MA (2003) Novel device for characterizing polymer flows in uniaxial extension. In: ANTEC '03 Soc Plastics Eng Tech Papers 49 (CD-ROM New York)
14. Sentmanat M (2003) Dual wind-up extensional rheometer. US Patent No. 6 578 413
15. Sentmanat M Dual (2004) Wind-up drum extensional rheometer. US Patent No. 6 691 569
16. Sentmanat M, Hatzikiriakos SG (in press) Rheol Acta
17. Sentmanat M, Wang B, McKinley GH (in press) J Rheol
18. Meissner J (1985) Chem Eng Commun 33:159–180
19. Laun HM, Schuch H (1989) J Rheol 33:119–175
20. Münstedt H, Kurzbeck S, Egersdörfer L (1998) Rheol Acta 37:21–29
21. McLeish TCB, Larson RG (1998) J Rheol 42:81–110
22. Sentmanat M, Hatzikiriakos SG (in press) Rheol Acta
23. Sentmanat M (2004)SER Universal Testing Platform—the ultimate in physical material characterization technology. In: ANTEC '04 Soc Plastics Eng Tech Papers 50 (CD-ROM New York)